

prepared for the  
National Institutes of Health  
National Institute of Neurological Disorders and Stroke  
Neural Prosthesis Program  
Bethesda, Maryland 20892

## **ELECTRODES FOR FUNCTIONAL ELECTRICAL STIMULATION**

**Contract #NO1-NS-6-2346**

**Progress Report #6  
April 1, 1998 - June 30, 1998**

**Principal Investigator  
J. Thomas Mortimer, Ph.D.**

**Applied Neural Control Laboratory  
Department of Biomedical Engineering  
Case Western Reserve University  
Cleveland, OH USA**

**THIS QPR IS BEING SENT TO  
YOU BEFORE IT HAS BEEN  
REVIEWED BY THE STAFF OF THE  
NEURAL PROSTHESIS PROGRAM.**

**TABLE OF CONTENTS**

<b>SECTION B. DESIGN AND FABRICATION OF ELECTRODES, LEADS AND CONNECTORS</b>	<b>3</b>
<b>B.2.1.2: Polymer-Metal Foil-Polymer (PMP) Cuff Electrodes</b>	<b>3</b>
<b>B.2.2: Lead Designs</b>	<b>7</b>
<b>B.2.4.1: Silicone Rubber Sheeting</b>	<b>8</b>
<b>B.2.4.2: Weld Strength</b>	<b>10</b>
<b>B.2.4.5: Cleaning Protocol</b>	<b>12</b>
<b>SECTION C. IN VIVO EVALUATION OF ELECTRODES</b>	<b>14</b>
<b>C.I.2.1.2: Electrode Selectivity: Sub-Fascicular</b>	<b>14</b>
<b>C.I.2.2: Selective Activation Stability Over Range and Time; Chronic Animal Tests</b>	<b>14</b>
<b>C.I.2.3: Continuous torque space</b>	<b>15</b>
<b>REFERENCES</b>	<b>20</b>

## SECTION B. DESIGN AND FABRICATION OF ELECTRODES, LEADS AND CONNECTORS

### B.2.1.2: Polymer-Metal Foil-Polymer (PMP) Cuff Electrodes

The polymer-metal foil-polymer (PMP) electrode is a novel design that attempts to improve the mechanical reliability and ease the manufacturing process of spiral nerve cuff electrodes. The electrode design uses laser micromachining technology to fabricate an electrode pattern in a polymer-metal foil laminate. During this reporting period, a second version of the electrode pattern is presently being implemented.

#### Previous Work

In period 5 a mass production of PMP2 electrodes was attempted. Results from steps 1 through 3 of the manufacturing process were shown in Progress Report #5. Continuation of the manufacturing process was to take place in period 6.

#### Current Work

In PR#5 we reported that we were having difficulty with the lamination process, at step 5 in the manufacturing process, causing distortion of the lead-contact pattern, as seen in Figure B.1.

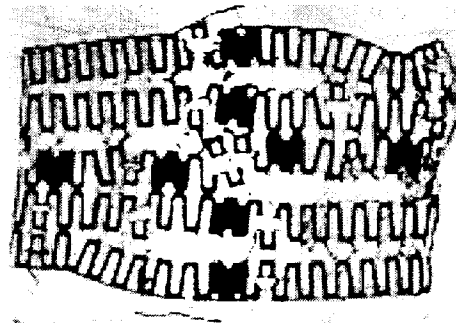


**Figure B.1:** The distortion of the platinum from a 3.45 mm cuff electrode is shown in the picture above. Expansion of the holes in the silicone rubber is the cause of most of the damage seen.

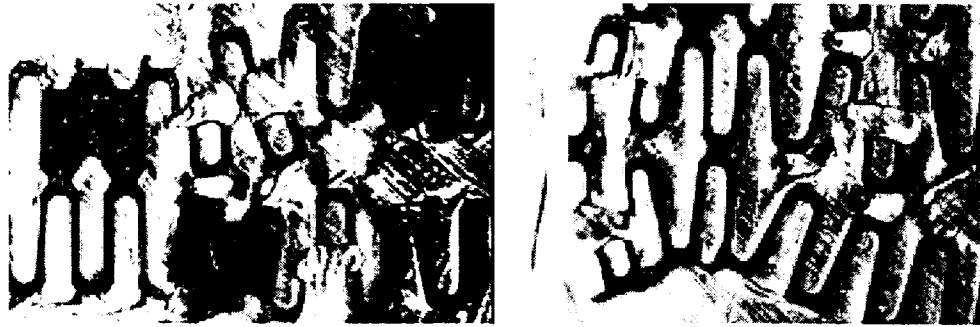


**Figure B.2:** Further magnification of the 3.45 mm cuff electrode shows the expansion and contraction of the silicone rubber and the holes in the electrode. The platinum also deformed its shape slightly due to the movement of the rubber.

It was hypothesized that the distortion of the pattern was a result of expansion of the holes in the silicone rubber when the viscous elastomer was being pushed into the holes faster than it could escape between the sheets of silicone. During this reporting period we have changed to a less viscous elastomer, NuSil's MED 6015, and slowed the pressing time in an effort to reduce the pressure on the holes in the laminated structure.

The application of the load was slowed by placing a spring on top of the lamination plates. This spring took the initial load of the press. In addition, because the spring constant was known, the load on the plates was obtained by measuring the distance the spring compressed. Testing using this apparatus was done to determine the load it takes for the elastomer to distribute and reach equilibrium. The load was applied in approximately 30 pound increments and the load was held for 30 minutes before the next addition. The distance that the lamination plates were separated was measured using a feeler gage. This measurement was taken before and after each load application. When the plate separation was equal to the final desired thickness, the elastomer was assumed to be in equilibrium and the full 2 ton load was applied. This test was performed using both the MED 4211 elastomer and the MED 6015 elastomer. It took the MED 4211 elastomer almost 3 hours and 400 pounds to reach equilibrium. On the other hand, it took the less viscous MED 6015 elastomer less than 30 minutes and only 30 pounds to reach equilibrium. The weight of the top plate alone was virtually enough for the elastomer to distribute completely.

After these results and careful examination of cuffs made with the MED 6015 elastomer, it was decided to change to the new elastomer. It was also decided that the spring and feeler gage would continue to be used to ensure that equilibrium is reached by the elastomer before full application of the load takes place. After this testing, another 3.45mm cuff electrode was attempted using the MED 6015 and the equilibrium technique. The results of this lamination are seen in the pictures below.

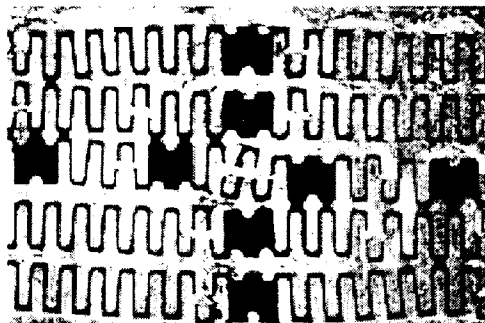


**Figure B.3:** A 3.45 mm cuff electrode was made using MED 6015 elastomer which has a much lower viscosity than the MED 4211 elastomer used previously. Some distortion in the silicone rubber can be seen. However, this electrode maintains its shape relative to the electrode pictures in Figures B.1 and B.2.

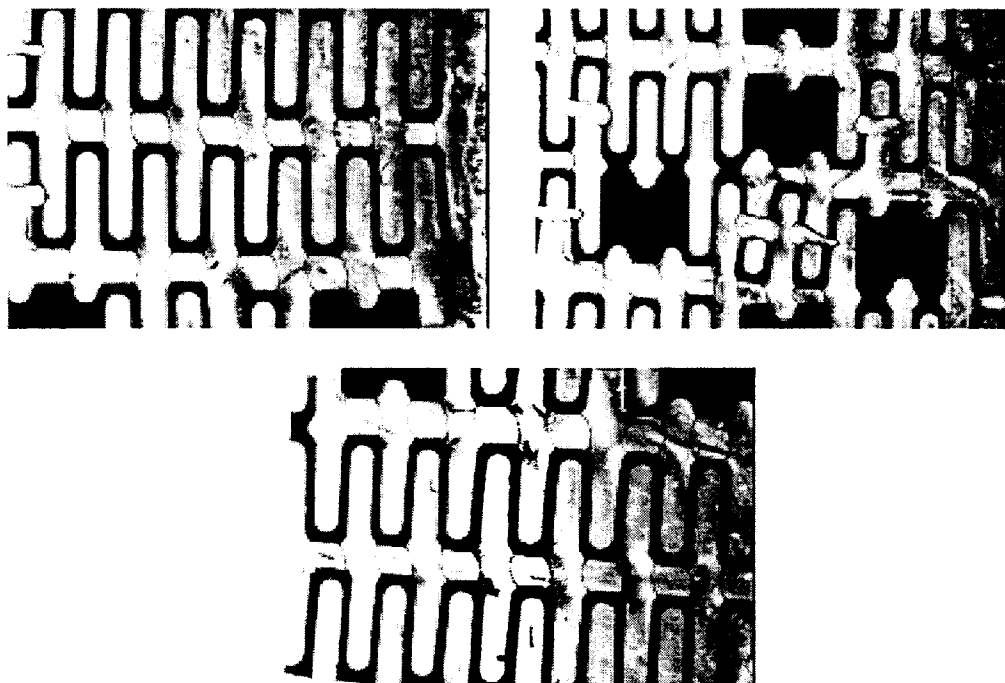


**Figure B.4:** Close-ups of the 3.45mm cuff electrode reveal only slight deformation of the silicone rubber holes. The largest amounts of deformation take place close to the pads and happen along rows of the holes through the platinum and silicone rubber.

Although some distortion of the intended pattern was still evident after using the new lamination procedure, it appears that the laminated assembly may still be suitable for implantation. During the next reporting period, we will be exploring a new hole pattern that should reduce distortion of even further.

During the course of manufacturing the spiral cuff electrodes we found that the diameters of the cuffs that were being produced were larger than expected and usually by a factor of two. Testing was pursued to determine a new formula for calculating the amount of stretch needed for a particular cuff diameter. The formula that we had been using was derived strictly according to geometry. It did not take into consideration the mechanical properties of the sheeting, elastomer, or platinum. It was thought that the correct stretch should be a scalar multiple of the stretch from the formula. In order to determine this, different stretches were attempted on a purely silicone rubber cuff. No platinum was included after early samples showed that there was little to no difference between the final diameters of cuffs with and without platinum. The testing began with the stretch required to make a 3.45mm cuff using a 0.002inch (50 $\mu$ m) stretched sheet and MED 6015 as the elastomer. Pictures of the resulting cuffs from tests using double, triple, and quadruple the normal amount of stretch are shown below.

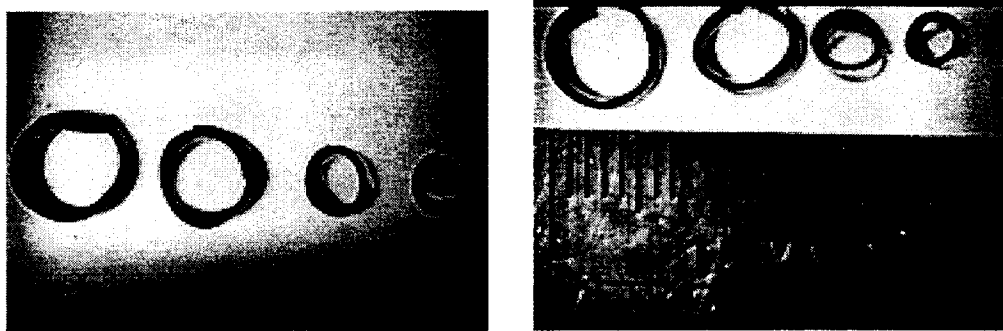


**Figure B.5:** These two pictures reveal the diameters of the cuffs made for the stretch calculations. More specifically, the spirals are the top views of the cuffs. The pictures are of intended 3.45mm cuffs using 1 times the stretch calculated from the formula, 2 times the stretch, 3 times the stretch, and 4 times the stretch. The relative actual diameters are: 6.75, 6.40, 3.25, and 2.33mm. The picture on the right shows the cuff size relative to a ruler. From this scale it is believed that the proper calculation for the stretch will be somewhere in between 2 and 3 times the calculated stretch.

Further, stretch calculations led to cuffs with 2.5 times the stretch from the original formula. Production of a 3.45mm cuff using 2.5 times the stretch yielded an actual diameter of 3.35mm. Production of a 2.55mm cuff using 2.5 times the stretch led to an actual diameter of 2.55mm. Both of these cuffs are considered accurate, therefore 2.5 times the stretch will be used for the production of cuffs using a 2 mil stretched sheet and MED 6015 elastomer. However, these tests will be repeated when we switch to 0.003inch (75 $\mu$ m) sheeting made with an elastomer base of MED 4550.

A 2.55mm cuff electrode was constructed using the old formula with a 2.5 multiplier; the resulting diameter was 2.55mm. This cuff did show some distortion and it did not have a smooth curl. This may be because the largest amount of stretch is used in the production of this cuff. That fact combined with the size of the weld and stimulation pads that resisted flexion resulted in a "bumpy" curl. Pictures of this cuff are shown below.

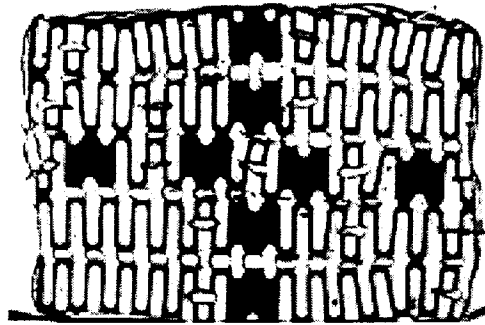


**Figure B.6:** The electrode shown was slightly damaged after the first lamination. Pictures of that were displayed in PR#5. Additional distortion occurred in the cuff lamination. Because the curl is tight for this electrode, flexion at the vertically aligned weld pads was difficult which yielded a “bumpy” curl.

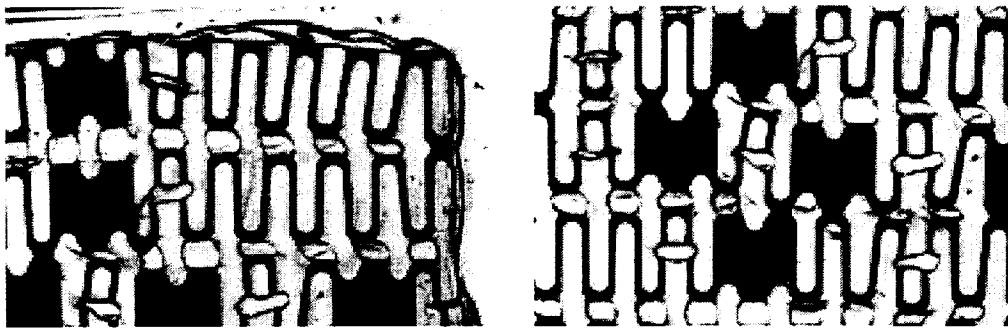


**Figure B.7:** Further magnification of the 2.55mm cuff electrode can be seen in the two pictures above. These close ups reveal the tension and compression of the holes in the silicone rubber.

### **Future Work**

Using the new MED 6015 elastomer, the plate separation technique, and the new stretch formula, the remaining PMP2 electrodes will be processed. We will also be working on a new electrode design that will employ fewer holes to define the conductivity paths, which should reduce the distortion during the lamination process. The new design will be called PMP3.

### **B.2.2: Lead Designs**

#### **Previous Work**

Testing of silicone rubber overcoated wire during period lead us to choose Specialty Silicone Fabricator's wire coated with NuSil's MED 4750 as the wire to be used to manufacture leads for the PMP electrodes.

### Current Work

During this reporting period we have examined coiled leads wound on mandrels that were .009, .012, .014, and .016 inches in diameter. A surfactant was used to ease the remove the wound coil from the mandrels and the resulting helixes were studied under an electron microscope. Pictures of the helixes are shown in the figure below. Note that all of the pictures were taken at the same magnification.

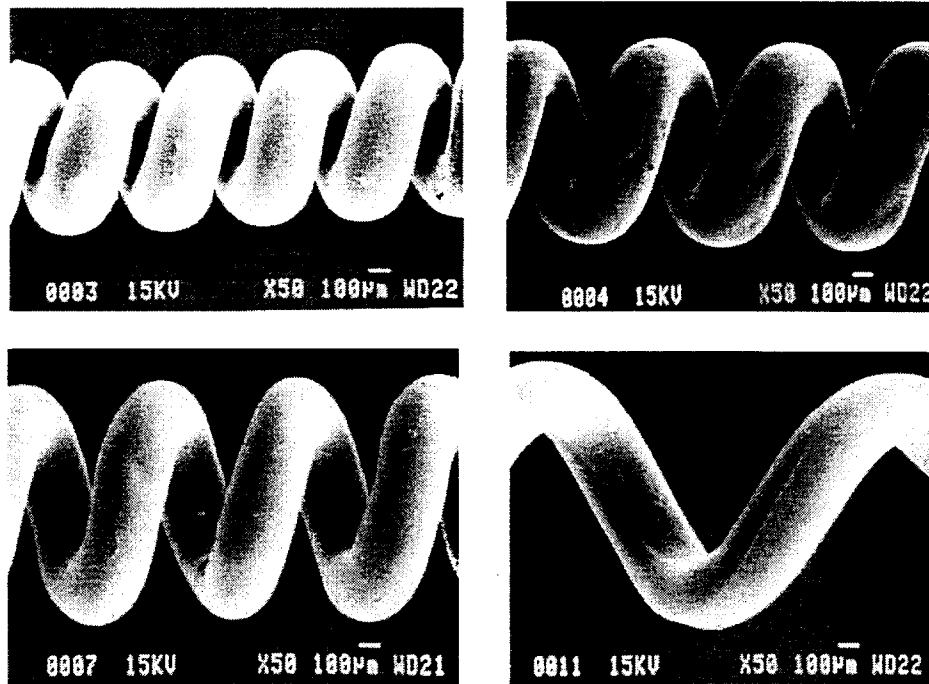


**Figure B.8:** Shown from top left to bottom right are coils formed by winding the silicone-fluoropolymer coated wire on , 0.009, 0.012, 0.014, and 0.016inch mandrels. Wire wound on the larger mandrels does not plastically deform to the same extent as the wire wound on the smaller mandrels and therefore tend to open after the coiling procedure.

The pictures above indicate that the desired shape for the helix can be achieved within the mandrel size range of 0.009 to 0.012 inch. Theoretically, the 0.011inch mandrel is the optimal size for winding this silicone rubber overcoated wire.

### Future Work

We will order 2,000 feet of the silicone overcoated wire to be used in lead manufacture.

#### B.2.4.1: Silicone Rubber Sheeting

The goal of this project is to establish performance specifications for the silicone rubber sheeting used in the spiral cuff electrode fabrication. Tests will be conducted to determine the mechanical and physical properties of four different silicone rubber sheeting formulations. Additionally, we will investigate the effects of aging and sterilization on these properties. All



specimens tested will have a thickness of 0.002inch (50µm). The control sample was supplied by Dow Corning and manufactured by AVECOR (Q7-4550.) This sheeting was used in the manufacture of our previous cuffs, but can no longer be used since it is not approved for long-term human implants. The new formulations are MED-4550, MED2-6640, and MED2-6641-1 and are supplied by NuSil and manufactured by Specialty Silicone Fabricators.

### **Current Work**

First, each specimen was cut with a scalpel blade into 3.5 x 0.3125inch rectangles. This size was chosen to conform to the ASTM D882-91 testing specification, the width of the specimens for tensile testing must be between 0.2 and 1.0inch. The width cannot be any smaller than 0.2inch because "narrow specimens magnify effects of edge strains or flaws" [ASTM D882-91]. During trial tests with the tensile testing machine, it was determined that because of the travel limitations of the machine, the width had to be less than 0.5inch in order for the specimen to fail. In addition, according to ASTM D882-91, the length has to be at least 2inches longer than the grip separation used (which is between 1 and 2inch.) Again because of the limitations on the machine, the longest specimen we could use, and still be within the specifications in the ASTM, was 3.5inch.

Once cut, the samples were put into three experimental groups – aged, sterilized, and control. Each sample was then cleaned according to the cleaning protocol in QPR# 4 (N01-NS-0-2395.) The aged group consisted of ten samples of each sheeting formulation which were placed in a saline bath at an elevated temperature to simulate five years aging in the body. The specimens were kept in the bath for 32 hours at 82°C [Larson et al. 1952]. The sterilized group consisted of ten samples of each formulation that underwent ethylene oxide (EO) sterilization. The control group consisted of ten samples from each formulation which were not put through any processing.

The first test each specimen underwent was a surface observation. The specimens were examined under a microscope to determine their surface properties. Moreover, their surface descriptions were recorded. This information may later help to explain irregular test results or patterns.

### **Future Work**

The next test the silicone rubber sheeting specimens will undergo will be a measure of their contact angle. A contact angle goniometer will be used to measure the advancing and receding water contact angles of each sample. These contact angles will tell us the hydrophobicity or hydrophilicity of the sheeting, which gives us an indication of the "stickiness" of the surfaces.

Upon completion of contact angle measurements, the specimens will undergo friction testing. The friction of each sample will be measured using a coefficient of friction testing fixture, which will be connected to a tensile testing machine. This fixture meets the requirements set forth in ASTM D1894-93. The silicone rubber sheeting samples will be attached to a rubber-covered surface of a 200-gram sled, which is drawn across a flat table covered with another silicone rubber sheeting sample. The sled is attached to a load cell, which will detect drag or friction. The coefficient of friction for a silicone rubber to silicone rubber interaction is determined from this test.

The final test to be performed is the tensile test, which will determine the modulus of elasticity, the ultimate tensile strength, the percent elongation, and the yield strength of each

specimen. The specimens will be cleaned and stored under a laminar flow hood between all tests.

From the results of these tests, a silicone rubber sheeting formulation will be chosen from the four tested. This sheeting will then be used for future electrode fabrication. This sheeting will be chosen according to desired results of a high tensile strength, a low coefficient of friction, and high hydrophobicity. The latter two are needed so that the cuffs will easily self-size. The results of the testing will also be used to determine performance specifications for future sheeting used for electrode fabrication.

#### **B.2.4.2: Weld Strength**

##### **Previous Work**

A special weld table was developed specifically for the PMP2 electrode. This table was illustrated in PR#5. Studies were done, using this new table, to determine the best weld settings for welding the leads onto the PMP2 electrode. It was found that a current of 1mA and a load of 50 ounces were the best settings.

##### **Current Work**

With the weld settings determined from the previous period's work, testing to determine the strength of the weld after lamination and simulated aging was done during this period. Three different groups of welds were tensile tested to failure. The first group was a control group that was a weld in the contact window of laminated platinum. The second group was pressed; meaning the weld was laminated and put in a heated press for 1 hour at 2 tons and 205°F. The last group was aged, after being pressed the laminated welds were soaked in an elevated temperature saline bath to simulate 5 years *in vivo*. A schematic of what the sample groups looked like is in Figure B.9.

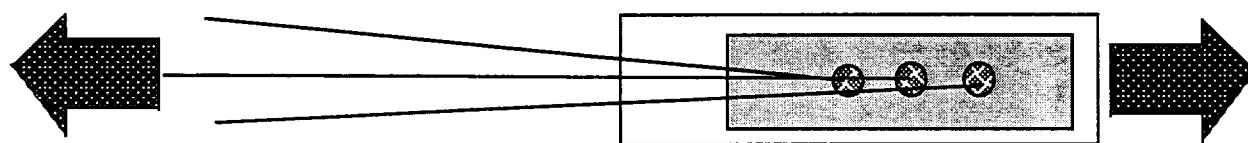


**Figure B.9** A piece of laminated platinum had weld ports cut with laser machining. Wires were then welded to the ports and the pressed and aged groups were encased in a silicone rubber lamination. The box surrounding the gray platinum represents the lamination. It can be seen from this picture that the welds and wires were covered by the lamination. These samples were tensile tested by gripping the platinum at the right end and gripping one of the wires on the other side.

The control group had an average peak load of 0.13597 N (SD=0.07146 , n=9). The pressed group could sustain an average peak load of 0.24525 N (SD=0.07835, n10) and the aged group could sustain an average peak load of 0.28809 N (SD=0.02293, n10). The results of this testing are shown in the chart below. The error bar shows the standard deviation for each group.

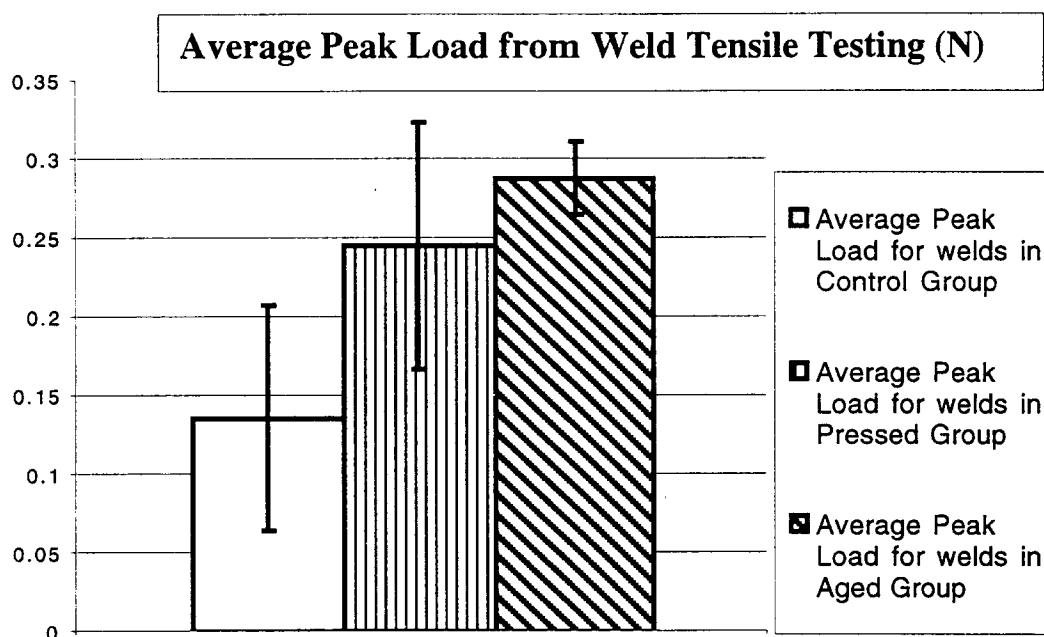


**Figure B.10.** The average peak loads (in Newtons) experienced by the welds tested in three groups. The error bars represent the standard deviations for each group. The lower error of the aged group is higher than the highest error for the control group. This leads to the conclusion that there is a statistical significance between the two groups. Tests for statistical significance are explained in the following text.

The yield strength of the laminated and the aged groups were greater than the yield strength of the control group. The differences were statistically significant at the 99.5% confidence level (Students "t" test, assuming the variances are unknown and unequal for each population tested). The difference between the yield strengths of the pressed and aged groups was not found to be significant at the 95% confidence level.

Microscopic examination of the welds after tensile testing revealed that wire adjacent to the weld site was failing rather than the weld itself. Under normal conditions, the breaking load of the wire is approximately 4.5 N, which is much higher than the breaking load of the wire in this testing. We interpret this difference to mean that the wire was weakened at the weld. Considering the yield strength measurements for the welded, laminated and aged groups along side the breaking strength of the wire, we conclude; 1) that the welding process reduces the strength of the wire at the site of the weld, 2) that the effect of the lamination process is to distribute some of the applied load to the non-welded parts of the assembly, and 3) that the simulated aging does not alter the weld strength.

**B.2.4.5: Cleaning Protocol**

The cleaning procedure we have been using on the spiral cuff electrodes involves multiple days of soaking in solutions of soapy water, ethanol, and pure water. This process is time consuming. During this reporting period, we have revisited the cleaning process, with the hope that we can improve the efficiency of the process without compromising the quality of cleaned product.

**Current Work**

The cleaning protocols that were studied were the current protocol for spiral cuff electrodes (reference), the current protocol for intramuscular electrodes (reference), and a new method that is a combination of the two methods. A control group, uncleaned electrodes, was also included in the study. All three cleaning protocols employ the use of the ultrasonic cleaner, Liquinox® (Alconox, Inc.), ethanol (reagent grade, Fisher Scientific), and ultrapure water (Milli-Q, Millipore). The only variations are time and soaking versus ultrasonic cleaning. The samples used to test the different processes were made without the platinum or lead wires. They were manufactured with a layer of silicone rubber stretched to a calculated value that yielded cuffs of a 3mm diameter. They were cut out of a sheet of the silicone rubber to have a cylindrical height of 6mm. The cuffs were cut to be a length that was equal to two wraps of the silicone rubber around itself. These samples were then cleaned according to a given protocol and then each was studied using electron microscopy. Pictures from the uncleaned samples and from the new method are shown below.

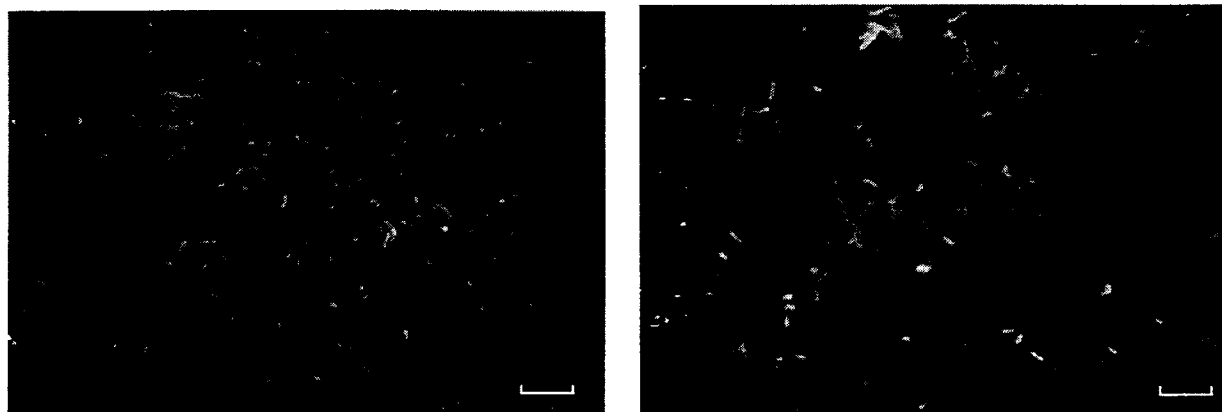


**Figure B.11:** Above are two pictures from two different samples of silicone rubber that were part of the control, uncleaned, group. Particulate matter can be seen on the surface of these samples. The picture on the left is a magnification of 50 and therefore the scale in the bottom right hand corner is equal to 2 $\mu$ m. The picture on the right has a magnification of 100 and therefore the scale is equal to 100 $\mu$ m.

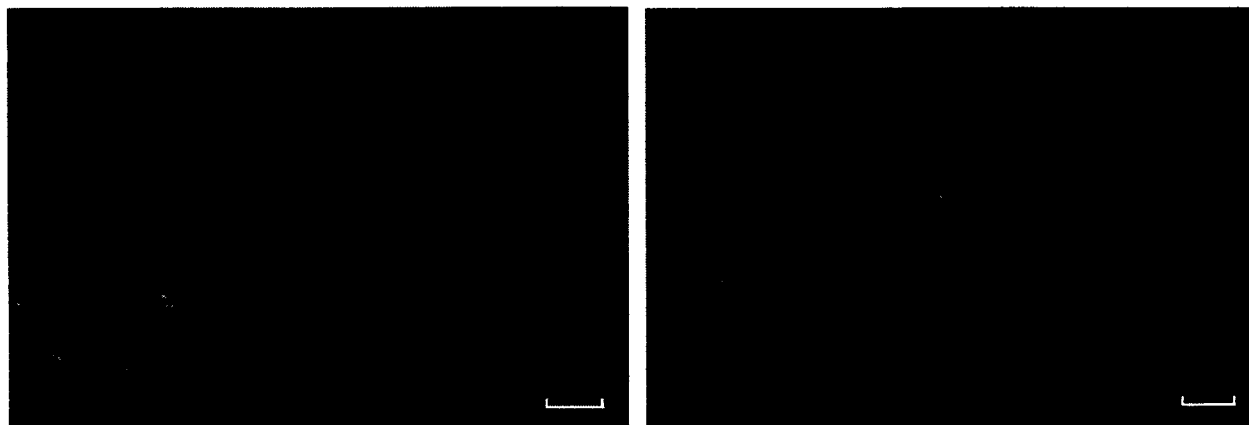


**Figure B.12:** The pictures above are of two samples that were cleaned using the new, shortened method. Only a small amount of particulate can be seen on the surface of these samples. The bars in the lower right hand corner are 100 $\mu$ m in length.

The samples cleaned with the shortened, new method met or exceeded the results from previous testing with the old method. Some of the factors that lead to this improvement are believed to be opening the cuff in the pure LiquiNox, the ultrapure water rinses after sonification, and the addition of heat to the process. The steps of the new method are listed below.

**Spiral Cuff Electrode Cleaning Protocol (new method):**

1. Dip the electrode in pure Liquinox® solution and separate the cuff layers to allow penetration of the solution into the cuffs.
2. Sonicate the electrode in a 1:100 solution of Liquinox® in ultrapure water for 10 minutes with the heat function on the ultrasonic cleaner turned on.
3. Rinse the electrode in ultrapure water 5 times.
4. Sonicate the electrode in ultrapure water for 5 minutes.
5. Sonicate the electrode in 95% ethanol for 5 minutes.
6. Rinse the electrode with ultrapure water 5 times.
7. Sonicate the electrode with ultrapure water for 5 minutes.
8. Allow the electrode to dry on the clean room wiper.
9. Package the electrode for sterilization.

This method is believed to be the best combination of effectiveness and efficiency and will therefore be used as the spiral cuff electrode cleaning protocol.

## **SECTION C. IN VIVO EVALUATION OF ELECTRODES**

### **C.I.2.1.2: Electrode Selectivity: Sub-Fascicular**

#### **Abstract**

Experiments performed during this reporting period have shown that field steering techniques can be employed to enhance selective activation at the sub-fascicular level. Sub-fascicular populations of nerve fibers contained within either the tibial or the common peroneal fascicles of the sciatic nerve were studied. A total of six animals have been studied thus far; the results of four experiments have been presented in previous reports, two experiments were performed during this period. The data from these two experiments are being analyzed at the time of this writing.

Our results to date include the separation of different sub-fascicular populations of axons in two of four animals. In one of the four animals, the results were inconclusive and the results from the fourth animal did not show any improvement.

### **C.I.2.2: Selective Activation Stability Over Range and Time; Chronic Animal Tests**

#### **Abstract**

The objective of this project is to qualify nerve cuff electrodes for use in human subjects. We have two designs that we believe are or will be technologically feasible and reliable, the PMP design and the wiggle-wire design. The first design, the PMP electrode, contains a sheet of platinum that is cut with a laser and embedded into the silicone rubber to produce a thin, multi-contact nerve cuff electrode. The wiggle-wire electrode is produced with the lead wires being bent back and forth in the plane of the electrode to allow the conductor to accommodate compression and tension during flexion of the cuff.

Chronic experiments designed to provide both histological data on the safety of these electrode designs and on the long-term stability of the recruitment properties of the electrodes were begun. We believe that in the chronic preparation, where the cuff electrode is stabilized with connective tissue, we can test additional techniques in an attempt to achieve sub-fascicular selectivity. The stability of the electrode was previously tested by Grill [1996] based on the change in the threshold value over time but the stability of more complicated electrode configurations were not tested. During the course of these experiments, we will test field steering techniques to verify that their properties also stabilize over time.

#### **Progress**

Two animals have been implanted, each with one four contact nerve cuff electrode. Testing on fascicular selectivity, sub-fascicular selectivity, and the range of torque output was started on one animal. We also plan to monitor the stability of the electrode and the stimulation properties. The data for the initial tests are presently being

processed. Based on the preliminary results, selective activation of three of the four fascicles were achieved using stimulation from a single contact and the fourth fascicle was achieved with the addition of anodic steering current from an adjacent contact.

### C.I.2.3: Continuous torque space

#### Abstract

The objective of this project is to develop methodologies, suitable for use with cuff electrodes, to effect contraction of multiple muscles, at different levels of activation, to produce any torque output in the physiological torque space. Activation of multiple muscles can be achieved using a field steering approach to shift the activated region between different muscles. Multiple muscle activation can also be achieved by using two different contacts stimulated with a short delay between the pulses to avoid field effects from the combination of pulses. The delay must be long enough to allow partially depolarized axons to return to their resting state but short enough to stay within the refractory period of the axons that were fully depolarized. In order to determine the necessary delay period, two animals were tested to assess the duration of both the hyper-excitable state and the refractory period of a nerve following the application of a stimulus pulse. We found that the hyper-excitable state lasted up to 500 $\mu$ s after the first pulse and the refractory period ended as early as 1300 $\mu$ s after the first pulse. A delay of 900 $\mu$ s was established as the standard that will be used between two independent stimulation pulses.

#### Progress

Experiments were carried out in two animals to determine: 1) the duration of the hyper-excitable state of the nerve fibers in the hind limb of cat following partial depolarization of the nerve and 2) the duration of the refractory state of the nerve fibers in the hind limb of cat following the initiation of an action potential. The tests performed on these animals were as follows:

- 1) Measure the torque-stimulus curve for each of the four contacts in the multi contact electrode using a 10  $\mu$ sec stimulus pulse. From these curves a stimulus current value, "test amplitude", was chosen that produced a sub-maximal torque from the muscles served by the fascicle with the lowest threshold.
- 2) Record the induced ankle torque on all three axes for the "test" stimulus, which establishes the base line torque for a single stimulus.
- 3) Record the induced ankle torque on all three axes when a two pulse sequence was applied to the electrode contact with each pulse being a 10  $\mu$ sec pulse at the "test" stimulus magnitude. Plot the recorded torque as a function of the delay between the first and second stimulus pulse.

An example of the results from one such test is shown in Figure C.1. On the x-axis is the time between the start of the two 10 $\mu$ s pulses. The baseline is shown at 1 and 2  $\mu$ s delays for stimulation by pulse 1 and 2 applied individually. Horizontal lines were drawn for the baseline plantar flexion, lateral rotation and eversion respectively from top to bottom. The two vertical lines indicate the end of the hyper-excitable period and the end of the refractory period. Using this particular contact and configuration, the boundaries of the purely refractory period were 70

and 3000 $\mu$ s. In figures C.2 and C.3 are shown graphs of 12 different runs from the two cats. The data shown in figures C.2 and C.3 have been normalized to the baseline torque produced by a single pulse. During the hyper-excitable phase, when the normalized torque is greater than one, the second pulse causes excitation of those fibers that were only partially depolarized by the first pulse. At times greater than the refractory period, when the normalized torque is again greater than one, the second pulse causes excitation of nerve fibers previously activated with the first pulse.. Negative values represent the recruitment of nerve fibers serving opposing muscles. In Cat #383 each contact on the sciatic and each of the branches were tested. There was no apparent difference between the refractory period of the contacts on the sciatic and the branches. The 0° contact is not shown due to the delay times not being recorded. The common peroneal branch is not shown due to a lack of data being acquired in the refractory region. All stimulation pulses used a 10 $\mu$ s pulse width except for the 'mg\_500' which used a 500 $\mu$ s pulse width to stimulate the medial gastrocnemius. No obvious difference was found between the 10 $\mu$ s and 500 $\mu$ s pulse width stimulation. The hyper-excitable period appeared to last up to 500 $\mu$ s and the end of the refractory period began around 3000 $\mu$ s after the first pulse. In figure C.3, Cat #388, five runs were performed on the four contacts on the sciatic. The hyper-excitable period appeared to last up to 450 $\mu$ s and the end of the refractory period appeared to begin around 1300 $\mu$ s after the first pulse. Considering data for both cats, the largest value for the hyper-excitable period was 500 $\mu$ s. The lowest value for the refractory period was 1300  $\mu$ s. Based on these results we recommend that a delay of 900  $\mu$ sec, between the application of pulses, be used to avoid residual field effects from stimuli applied to other electrodes in a multi-contact cuff. These results also indicate that the upper frequency for a multiplexed system is 2 kHz to avoid interacting residual field effects.



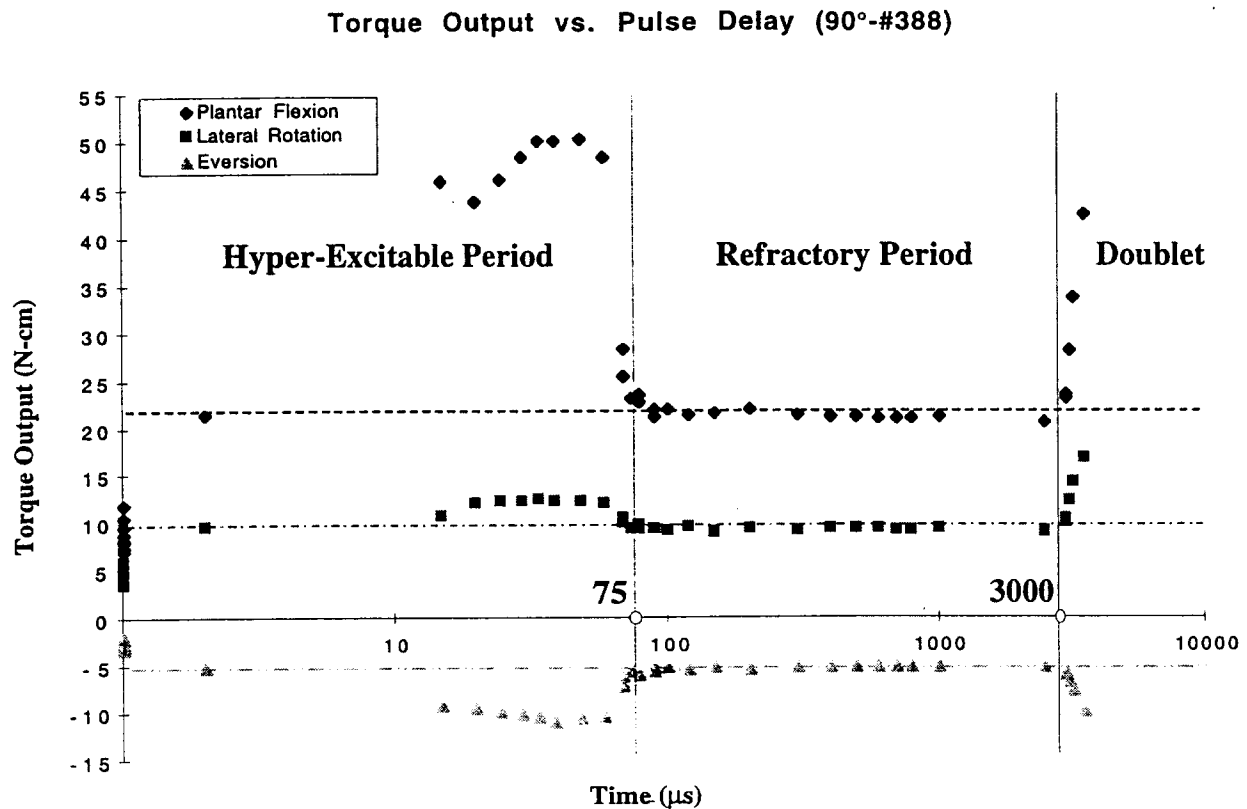


**Figure C.1** – Torque output as a function of time between two pulses. The torque output of a single pulse alone is shown on the graph located at a time delay of 1 and 2  $\mu$ s for the first and second pulses respectively. The baseline values for plantar flexion, lateral rotation and eversion are shown by horizontal lines from top to bottom respectively. At times less than 75 $\mu$ s the electrical fields added to produce excitation of nerve fibers that are not excited by only one of the pulses (hyper-excitable period). At times greater than 3000 $\mu$ s, nerve fibers that were activated with the first pulse are activated again by the second pulse signifying the end of the refractory period.

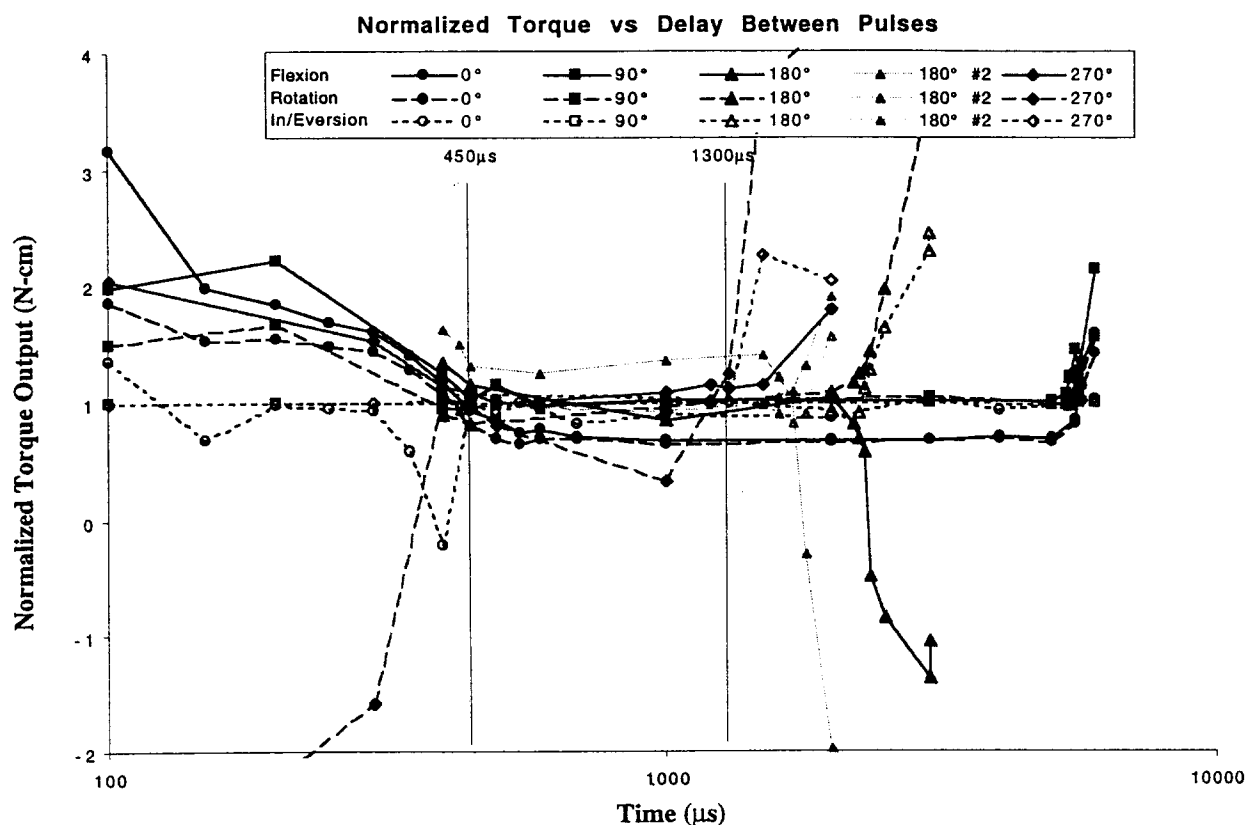


**Figure C.2** – Normalized torque output as a function of time between two pulses for seven different runs with Cat #383. The torque output was normalized by the torque output of a single pulse alone. The 0° contact is not shown since the delay times were not recorded. Sufficient data was not taken for the CP. All stimulation used a 10 $\mu$ sec pulse except for 'mg\_500' which used a 500 $\mu$ s pulse. Times less than 500 $\mu$ s were determined to be within the hyper-excitable period. Times greater than 3000 $\mu$ s were determined to be beyond the refractory period.

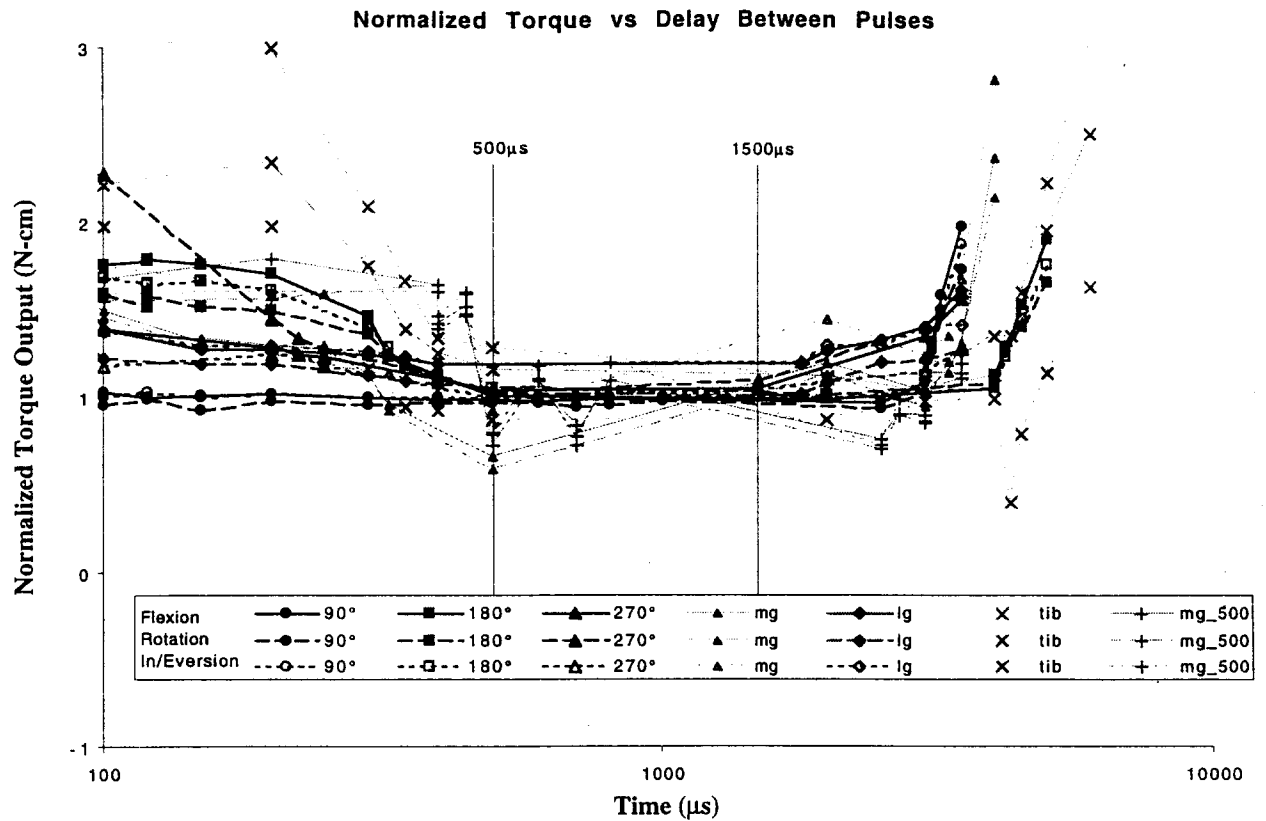


**Figure C.3** – Normalized torque output as a function of time between two pulses for seven different runs with Cat #388. The torque output was normalized by the torque output of a single pulse alone. Times less than 450μs were determined to be within the hyper-excitable period. Times greater than 1300μs were determined to be beyond the refractory period.

## REFERENCES

Johnson, Norman L. and Leone, Fred C., Statistics and Experimental Design in Engineering and the Physical Science, vol. 1, John Wiley and Sons, Inc.; New York, 1964.

Larson, F.R. and Miller, James, "A Time-Temperature Relationship for Rupture and Creep Stresses", *Trans ASME*, vol. 74, p. 767, 1952.

"Standard Test Methods for Tensile Properties of Thin Plastic Sheeting", ASTM D-882, p.183, 1991.